Journal of Magnetism and Magnetic Materials 515 (2020) 167262

Contents lists available at ScienceDirect

Journal of Magnetism and Magnetic Materials

journal homepage: www.elsevier.com/locate/jmmm

Research articles

Structure, magnetic and thermodynamic properties of heterometallic ludwigites: Cu_2GaBO_5 and Cu_2AlBO_5

R.M. Eremina[a,*], T.P. Gavrilova[a], E.M. Moshkina[b], I.F. Gilmutdinov[c], R.G. Batulin[c], V.V. Gurzhiy[d], V. Grinenko[e,f], D.S. Inosov[f]

[a] Zavoisky Physical-Technical Institute, FRC Kazan Scientific Center of RAS, Sibirsky tract, 10/7, Kazan 420029, Russia
[b] Kirensky Institute of Physics, Federal Research Center KSC SB RAS, 660036 Krasnoyarsk, Russia
[c] Institute of Physics, Kazan Federal University, 420008 Kazan, Russia
[d] Department of Crystallography, Institute of Earth Sciences, St. Petersburg State University, University Emb. 7/9, 199034 St. Petersburg, Russia
[e] Leibniz Institute for Solid State and Materials Research, IFW Dresden, 01069 Dresden, Germany
[f] Institute for Solid State and Materials Physics, TU Dresden, 01069 Dresden, Germany

ARTICLE INFO

Keywords:
Crystal structure
Ludwigite
Quasi-one-dimensional magnetism
Antiferromagnetic order
Specific heat
Magnetization

ABSTRACT

We present an extensive study of the structural, magnetic and thermodynamic properties of high-quality monocrystals of two heterometallic oxyborates from the ludwigite family: Cu_2GaBO_5 and Cu_2AlBO_5 in the temperature range above 2 K. The distinctive feature of the investigated structures is the selective distribution of Cu and Ga/Al cations. The unit cell of Cu_2GaBO_5 and Cu_2AlBO_5 contains four nonequivalent crystallographic sites of metal ions. Two sites in the structure of Cu_2GaBO_5 are fully occupied by Cu atoms which form the quasi one-dimensional chains along the *a*-axis. For Cu_2AlBO_5 all sites are partially occupied by Al and Cu atoms. The joint analysis of low-temperature data on magnetic susceptibility and magnetic contribution to the specific heat showed that Cu_2AlBO_5 and Cu_2GaBO_5 exhibit an antiferromagnetic transition at T_N = 2.4 and 4.1 K, respectively. The magnetic response below T_N can be represented as the sum of two contributions: the ordered component and the paramagnetic contribution from defects of the same relative weight. It is shown that the external magnetic field above 2.5 T and 2.8 T for Cu_2GaBO_5 and Cu_2AlBO_5, respectively, leads to a broadening of the magnetic phase transition indicating suppression of the long-range antiferromagnetic order.

1. Introduction

Cu_2GaBO_5 and Cu_2AlBO_5 oxyborates belong to the ludwigite family with the general formula $M_2^{2+}M'^{3+}BO_5$, where *M* and *M'* are divalent and trivalent metal ions, respectively. During the last twenty years a lot of works were devoted to the investigations of bimagnetic ludwigites Cu_2MnBO_5 [1–3], $Mn_{3-x}Ni_xBO_5$ [4], Cu_2FeBO_5 [5,6], Ni_2FeBO_5 [7,8], Co_2FeBO_5 [8] and others. Usually the investigations of ludwigites start from the detailed sample characterization, because the final sample composition can differ from the composition of the corresponding mixture of the starting components. In addition to the structural data, the magnetization [2–5,7,8], specific heat [2,8], neutron powder diffraction [2], Mössbauer spectroscopy [5,7] measurements, and the calculations of the exchange integrals in frameworks of the indirect coupling model [1,6] are presented in the literature.

Magnetic properties of oxyborates with the ludwigite structure are usually related with the presence of zigzag walls in their crystal structure formed by metal ions of different valency and also the presence of up to twelve magnetic ions in the unit cell, which occupy four nonequivalent positions. Usually the copper-containing ludwigites are characterized by the antiferromagnetic or ferrimagnetic ordering with low value of the uncompensated magnetic moment and low temperature of magnetic ordering.

Partial substitution of copper ions with Co^{2+} cations and occupation of trivalent positions with Al^{3+} cations leads to a significant anisotropy of the magnetic properties in $CuCoAlBO_5$ [9]. Authors suggested that such a difference is due to the influence of the strong spin–orbit coupling of Co^{2+} ions, which leads to the canting of the magnetic moments on neighboring sublattices and causes a weak spontaneous magnetic moment [9]. Unlike other Cu-containing oxyborates, $Co_{2.88}Cu_{0.12}BO_5$ is the highly anisotropic hard ferrimagnet with a large uncompensated moment [10]. However, the comparison of magnetic properties of $Co_{2.88}Cu_{0.12}BO_5$ ludwigite with homometallic Co_3BO_5 showed that the replacement of cobalt ions with copper does not affect the magnetic

* Corresponding author.
E-mail address: REremina@yandex.ru (R.M. Eremina).

https://doi.org/10.1016/j.jmmm.2020.167262
Received 7 May 2020; Received in revised form 25 June 2020; Accepted 24 July 2020
Available online 05 August 2020
0304-8853/ © 2020 Elsevier B.V. All rights reserved.

properties of the sample: a slight decrease in the macroscopic magnetic moment and invariability of the ferrimagnetic ordering temperature (T_N = 43 K) were observed [10]. The $Cu_{3-x}Mn_xBO_5$ ($x = 2$) ludwigite is characterized by the ferrimagnetic ordering below T_N = 92 K demonstrating a possible increase in the macroscopic magnetic moment and the magnetic ordering temperature in ludwigites [11]. A completely different picture of phase transitions is observed in Cu_2FeBO_5 ludwigite, where the phase transition of the iron subsystem from the paramagnetic to the spin glass state was observed at $T = 63$ K, the Cu^{2+} subsystem passes into a magnetically ordered state at $T_{N1} = 38$ K, and only below $T_{N1} = 20$ K the sample is fully ordered [12].

Magnetic measurements and the analysis of exchange interactions in Cu_2FeBO_5 and Cu_2GaBO_5 showed that these compounds are antiferromagnetic (AFM) with Néel temperatures of 32 and 3 K, respectively [5,12]. The authors concluded that the magnetic properties of this type of compounds are substantially dependent on the degree of cation distribution over crystallographic positions. As follows from Ref. [12], Cu_2GaBO_5 is a low-dimensional magnetic system, for which magnetic transition to an antiferromagnetically ordered state was observed in the temperature dependence of magnetic susceptibility. A definitive answer can only be given by studying the temperature dependence of magnetic susceptibility on alternating current (AC) [13], which has not yet been carried out for the Cu_2GaBO_5 single crystal. The details of the synthesis process of Cu_2AlBO_5 ludwigite were previously reported [14], but the magnetic properties of this compound have not been investigated until now. The temperature dependencies of the specific heat were not obtained for Cu_2AlBO_5 and Cu_2GaBO_5.

Here we present the detailed investigations of structural, magnetic and thermodynamic properties of Cu_2GaBO_5 and Cu_2AlBO_5 ludwigites, which contain only one type of magnetic ion Cu^{2+}. We suggest that these investigations will help in understanding the type of the magnetic ordering in the homomagnetic heterometallic ludwigites.

2. Experimental methods and results

2.1. Sample preparation

Here we present the physical properties measurements of Cu_2GaBO_5 and Cu_2AlBO_5 single crystals, synthesized by the flux technique. The grown single crystals of Cu_2GaBO_5 and Cu_2AlBO_5 ludwigites were in the form of dark-green prisms up to $3 \times 4 \times 15$ and $1 \times 1 \times 10\,mm^3$ in size, respectively. The long side of the prism coincides with the crystallographic *a*-direction. Details of the synthesis process are given in Ref. [15].

2.2. Chemical composition

Small fragments of Cu_2GaBO_5 (**1**) and Cu_2AlBO_5 (**2**) were crushed, pelletized, and carbon coated. The chemical compositions of the samples were determined using a Hitachi TM 3000 scanning electron microscope equipped with an EDX spectrometer. Analytical calculations **1**: Atomic ratio from structural data Cu 1.96, Ga 1.04; found by EDX: Cu 1.95, Ga 1.05. Analytical calculations **2**: Atomic ratio from structural data Cu 1.82, Al 1.18; found by EDX: Cu 1.84, Al 1.16.

In spite of the real atomic ratio Cu:Ga (or Cu:Al) is not 2:1 in the investigated samples, in this work we use the ideal formula Cu_2GaBO_5 and Cu_2AlBO_5 instead $Cu_{2.05}Ga_{0.95}BO_5$ and $Cu_{1.81}Al_{1.19}BO_5$.

2.3. Single-crystal X-ray diffraction study

Crystal structures of **1** and **2** were determined by the means of single-crystal X-ray diffraction analysis. Crystals were selected under an optical microscope, encased in oil-based cryoprotectant, and fixed on micro mounts. Diffraction data for **1** were collected at 293 K using a Bruker SMART diffractometer equipped with an APEX II CCD area detector operated with monochromated MoK_α radiation (λ[MoK_α] = 0.71073 Å) at 40 kV and 30 mA. Data were collected with frame widths of 1.0° in ω and φ, and an exposure of 2 s per frame. Data were integrated and corrected for background, Lorentz, and polarization effects by means of the Bruker programs *APEX2* and *XPREP*. Absorption correction was applied using the empirical spherical model within the *SADABS* program [16]. Diffraction data for **2** were collected at 293 K using a Rigaku Oxford Diffraction Xcalibur diffractometer operated with monochromated MoK_α radiation (λ[MoK_α] = 0.71073 Å) at 50 kV and 40 mA and equipped with an Eos CCD area detector. Data were collected with frame widths of 1.0° in ω and φ, and an exposure of 2 s per frame. Data were integrated and corrected for background, Lorentz, and polarization effects. An empirical absorption correction based on spherical harmonics implemented in the SCALE3 ABSPACK algorithm was applied in *CrysAlisPro* program [17]. The unit cell parameters of **1** and **2** (Table 1) were determined and refined by least-squares techniques. The structures were solved by direct methods and refined using the *SHELX* program [18] incorporated in the *OLEX2* program package [19]. The final models included coordinates, see Table 2, and anisotropic displacement parameters for all atoms. Selected interatomic distances are listed in Table 3. It should be noted that in some cases highly redundant XRD data (full sphere and $I/\sigma > 30$–40) allow refining the site occupancy factors for close, even neighbor, elements from the Periodic Table [20]. Supplementary crystallographic data have been deposited in the Inorganic Crystal Structure Database (CSD 1884474 (**1**) and 1884475 (**2**)) and can be obtained from the Cambridge Crystallographic Data via https://www.ccdc.cam.ac.uk/structures/.

Table 1
Crystallographic data for Cu_2GaBO_5 (**1**) and Cu_2AlBO_5 (**2**).

Compound	1	2
Formula	$Cu_{2.05}Ga_{0.95}BO_5$	$Cu_{1.81}Al_{1.19}BO_5$
Crystal system	monoclinic	monoclinic
a (Å)	3.1121(1)	3.0624(2)
b (Å)	11.9238(3)	11.7855(6)
c (Å)	9.4708(2)	9.3747(6)
α (°)	90	90
β (°)	97.865(1)	97.737(5)
γ (°)	90	90
V (Å^3)	348.137(16)	335.27(4)
Molecular weight	287.87	238.11
Space group	$P2_1/c$	$P2_1/c$
μ (mm^{-1})	19.595	11.742
Temperature (K)	293(2)	293(2)
Z	4	4
D_{calc} (g/cm^3)	5.481	4.717
Crystal size (mm^3)	0.18×0.14×0.09	0.22×0.16×0.10
Diffractometer	Bruker Smart Apex II	Rigaku Oxford Diffraction Xcalibur Eos
Radiation	MoK_α	MoK_α
Total reflections	9729	1711
Unique reflections	1873	761
Angle range 2Θ (°)	5.53–79.20	5.58–55.00
Reflections with $\|F_o\| \geqslant 4F$	1755	694
R_{int}	0.0394	0.0437
R_σ	0.0264	0.048
R_1 ($\|F_o\| \geqslant 4F$)	0.0181	0.0299
wR_2 ($\|F_o\| \geqslant 4F$)	0.0394	0.0636
R_1 (all data)	0.0209	0.0323
wR_2 (all data)	0.0402	0.0660
S	1.114	1.047
ρ_{min}, ρ_{max} (e/Å^3)	−0.715, 0.883	−0.820, 0.928
ICSD	1884474	1884475

$R_1 = \Sigma||F_o| - |F_c||; wR_2 = \{\Sigma[w(F_o^2 - F_c^2)^2]/\Sigma[w(F_o^2)^2]\}^{1/2}; w = 1/[\sigma^2(F_o^2) + (aP)^2 + bP]$; where $P = (F_o^2 + 2F_c^2)/3; S = \{\Sigma[w(F_o^2 - F_c^2)]/(n-p)\}^{1/2}$, where *n* is the number of reflections and *p* is the number of refinement parameters.

Table 2
Atomic coordinates, isotropic displacement parameters (Å^2) and site occupancy factors (s.o.f.) for Cu_2GaBO_5 (**1**) and Cu_2AlBO_5 (**2**).

Atom	*x*	*y*	*z*	U_{eq}	s.o.f.
			1		
Cu1	0.46491(6)	0.71961(2)	0.50724(2)	0.00621(6)	1
Cu2	0.500000	0.500000	1.000000	0.00497(6)	1
Ga3	0.000000	0.500000	0.500000	0.00490(8)	0.66
Cu3	0.000000	0.500000	0.500000	0.00490(8)	0.34
Cu4	0.92862(5)	0.61907(2)	0.77187(2)	0.00601(6)	0.29
Ga4	0.92862(5)	0.61907(2)	0.77187(2)	0.00601(6)	0.71
B1	0.9641(5)	0.86426(11)	0.73488(17)	0.0051(2)	1
O1	0.4585(4)	0.64426(8)	0.89925(12)	0.00934(19)	1
O2	1.0289(3)	0.46141(8)	0.84306(11)	0.00658(16)	1
O3	0.9152(3)	0.76255(8)	0.66705(11)	0.00808(18)	1
O4	0.0074(3)	0.63394(8)	0.38096(12)	0.00685(17)	1
O5	0.5519(7)	0.57364(15)	0.6018(2)	0.0068(3)	0.63
O5A	0.4148(12)	0.5856(3)	0.6286(4)	0.0068(3)	0.37
			2		
Cu1	0.46022(14)	0.71962(4)	0.50700(5)	0.0070(2)	0.88
Al1	0.46022(14)	0.71962(4)	0.50700(5)	0.0070(2)	0.12
Cu2	0.500000	0.500000	1.000000	0.0058(3)	0.86
Al2	0.500000	0.500000	1.000000	0.0058(3)	0.14
Cu3	0.000000	0.500000	0.500000	0.0062(4)	0.34
Al3	0.000000	0.500000	0.500000	0.0062(4)	0.66
Cu4	0.9285(2)	0.61643(6)	0.76921(8)	0.0065(3)	0.33
Al4	0.9285(2)	0.61643(6)	0.76921(8)	0.0065(3)	0.67
B1	0.9632(14)	0.8634(3)	0.7353(5)	0.0093(9)	1
O1	0.4583(10)	0.6440(2)	0.8951(4)	0.0196(8)	1
O2	1.0139(7)	0.4617(2)	0.8422(3)	0.0116(7)	1
O3	0.9147(8)	0.7604(2)	0.6692(3)	0.0129(7)	1
O4	–0.0045(8)	0.6327(2)	0.3830(3)	0.0117(7)	1
O5	0.562(2)	0.5695(5)	0.6011(7)	0.0130(12)	0.58
O5A	0.392(3)	0.5835(7)	0.6295(11)	0.0130(12)	0.42

Table 3
Selected bond lengths in the crystal structure of Cu_2GaBO_5 and Cu_2AlBO_5.

Cu_2GaBO_5			Cu_2AlBO_5		
Bond	Bond length (Å)		Bond	Bond length (Å)	
Cu1–O1		1.9172(10)	Cu1(Al1)–O1		1.919(3)
Cu1–O3		1.9840(10)	Cu1(Al1)–O3		1.977(2)
Cu1–O4		2.4241(11)	Cu1(Al1)–O4		2.366(3)
Cu1–O4		2.0087(10)	Cu1(Al1)–O4		1.995(3)
Cu1–O5		1.9591(18)	Cu1(Al1)–O5		1.983(6)
Cu1–O5A		1.987(3)	Cu1(Al1)–O5A		2.000(9)
⟨Cu1–O⟩		2.047	⟨Cu1(Al1)–O⟩		2.040
Cu2–O1	2×	1.9627(10)	Cu2(Al2)–O1	2×	1.957(3)
Cu2–O2	2×	1.9935(10)	Cu2(Al2)–O2	2×	2.004(3)
Cu2–O2	2×	2.4082(11)	Cu2(Al2)–O2	2×	2.344(3)
⟨Cu2–O⟩		2.122			2.102
Cu3(Ga3)–O4	2×	1.9569(10)	Cu3(Al2)–O4	2×	1.909(3)
Cu3(Ga3)–O5	2×	2.0485(18)	Cu3(Al2)–O5	2×	1.927(7)
Cu3(Ga3)–O5	2×	2.003(2)	Cu3(Al2)–O5	2×	2.022(6)
Cu3(Ga3)–O5A	2×	1.939(3)	Cu3(Al2)–O5A	2×	1.869(10)
⟨Cu3(Ga3)–O⟩		1.986	⟨Cu3(Al3)–O⟩		1.932
Cu4(Ga4)–O1		2.0419(13)	Cu4(Al4)–O1		2.007(3)
Cu4(Ga4)–O1		1.9287(11)	Cu4(Al4)–O1		1.901(3)
Cu4(Ga4)–O2		2.0071(10)	Cu4(Al4)–O2		1.953(3)
Cu4(Ga4)–O3		1.9756(10)	Cu4(Al4)–O3		1.936(3)
Cu4(Ga4)–O5		1.9357(18)	Cu4(Al4)–O5		1.891(7)
Cu4(Ga4)–O5A		2.203(4)	Cu4(Al4)–O5A		1.996(10)
Cu4(Ga4)–O5A		1.991(3)	Cu4(Al4)–O5A		2.095(10)
⟨Cu4(Ga4)–O⟩		2.012	⟨Cu4(Al4)–O⟩		1.968
B1–O2		1.3754(17)	B1–O2		1.374(5)
B1–O3		1.3711(18)	B1–O3		1.362(5)
B1–O4		1.3717(19)	B1–O4		1.376(5)
⟨B1–O⟩		1.373	⟨B1–O⟩		1.371

2.4. Magnetic susceptibility

The magnetization *M* of single crystalline samples was measured on the commercial Physical Properties Measurements System (PPMS-9 device) within a temperature range 2 K⩽ T ⩽400 K in field-cooled (FC) and zero-field-cooled (ZFC) regimes in magnetic fields H up to 9 T. Fig. 1 shows the FC magnetic susceptibility $\chi = M/H$ of Cu_2GaBO_5 and Cu_2AlBO_5 ludwigites as a function of temperature for the magnetic field applied parallel and perpendicular to the crystallographic *a*-axis. Fig. 2 shows the temperature dependence of magnetic susceptibility $\chi = M/H$ measured in ZFC and FC regimes at low temperatures. The magnetic phase transition temperature was obtained as the susceptibility anomaly which corresponds to the splitting temperature of ZFC and FC curves: T = 4.1 K for Cu_2GaBO_5 and T = 2.4 K for Cu_2AlBO_5, respectively (Fig. 2), that is in agreement with our previously published results [21]. One can see that the magnetic phase transition is less visible in Cu_2AlBO_5 in respect to Cu_2GaBO_5 that can be due to more randomly distributed magnetic ions over the Cu_2AlBO_5 structure. The obtained temperature for Cu_2GaBO_5 is different from the previously observed Néel temperature T_N = 3.4 K in Ref. [12], where temperature dependencies of the magnetization were measured in a magnetic field of 50 Oe in contrast with the presented here measurements in a magnetic field of H = 1 κOe. The difference in Néel temperatures can result from the quality of the sample and different distribution of metal ions among four nonequivalent positions in the unit cell, or from the destruction of the AFM order by a sufficiently weak magnetic field.

It is possible to unambiguously indicate the type of magnetic phase transition only by studying the temperature dependence of the

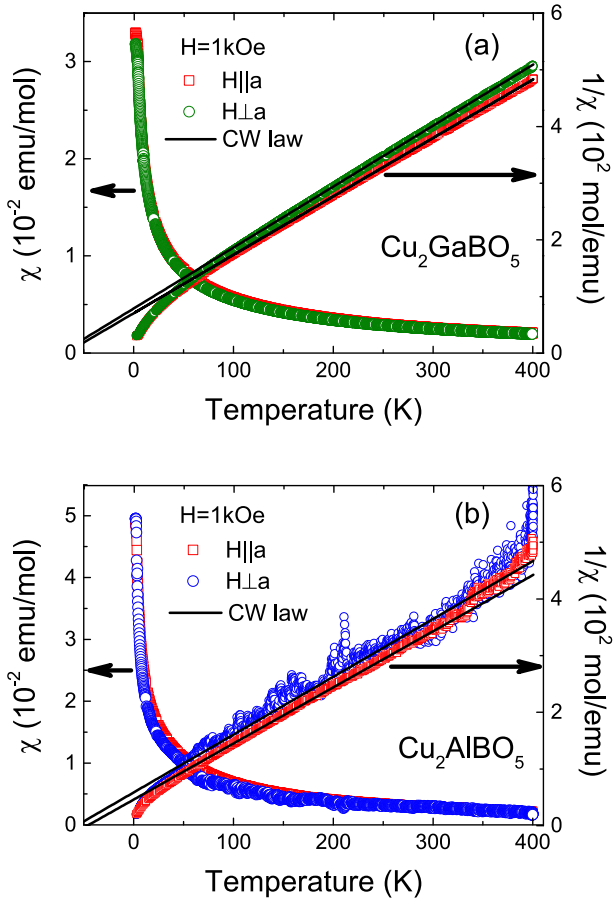


Fig. 1. Temperature dependencies of the magnetic susceptibility and inverse magnetic susceptibility in (a) Cu_2GaBO_5 and (b) Cu_2AlBO_5 ludwigites measured in FC regime in the magnetic field (H = 1 κOe) applied parallel and perpendicular to the crystallographic *a* axis.

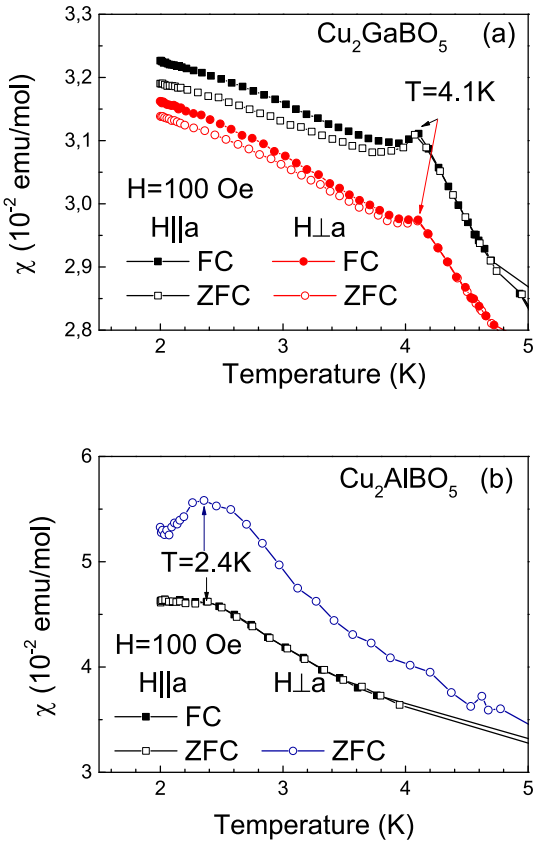


Fig. 2. Temperature dependence of the magnetic susceptibility at low temperatures measured in FC and ZFC regimes in (a) Cu_2GaBO_5 and (b) Cu_2AlBO_5 ludwigites in the magnetic field (H = 100 Oe) applied parallel and perpendicular to the crystallographic a axis.

magnetization on alternating current. Fig. 3 presents the temperature dependence of the AC magnetic susceptibility measured with H_{AC} = 4 Oe. The presence of a peak in the real part of the magnetization and its absence in the imaginary part of the magnetization indicates the transition from an antiferromagnetic to the paramagnetic state for Cu_2GaBO_5 single crystal at 4.1 K. The magnetic field dependence of the magnetization for Cu_2GaBO_5 and Cu_2AlBO_5 is presented in Fig. 4.

2.5. Specific heat

The specific heat was measured by the relaxation method using a Physical Property Measurement System (PPMS) (Quantum Design) in the temperature range 1.8 K$<T<$400 K and in magnetic fields up to 13.8 T. Fig. 5 shows the specific heat $C(T)$ as a function of temperature for Cu_2GaBO_5 and Cu_2AlBO_5 ludwigites measured in zero magnetic field. An anomaly was observed in the $C(T)$ data at T = 4.1 K and $T \approx$ 3 K in Cu_2GaBO_5 and Cu_2AlBO_5, respectively (inset in Fig. 5a). The obtained value is coincide with the corresponding anomaly in the $\partial\chi/\partial T$ vs. T curve for Cu_2GaBO_5. One can suggest that the small difference between phase transition temperatures obtained from magnetization and specific heat data for Cu_2AlBO_5 can be due to the different orientation of the sample during these experiments, because Cu_2AlBO_5 has a more pronounced angular dependence of the magnetic properties in respect to Cu_2GaBO_5 or this difference may be due to the destruction of the magnetic order by an external magnetic field during the magnetization measurements in Cu_2AlBO_5. In the accessible magnetic-field range, the anomaly is field dependent, indicating the broadening and the decreasing of the peak intensity with increasing of the applied magnetic field (Fig. 6). This suggests that the small magnetic field (on the order of 2.5 T) destroys of the long-range AFM order.

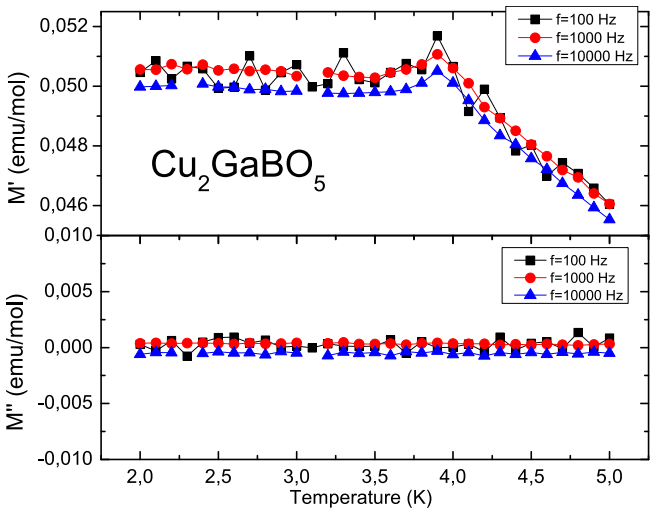


Fig. 3. Temperature dependence of the real and imaginary parts of the AC magnetization as a function of frequency at low temperatures for H = 4 Oe in Cu_2GaBO_5.

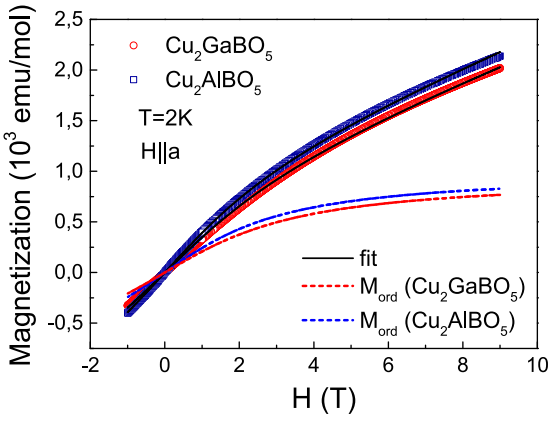


Fig. 4. Magnetic field dependence of the magnetization of Cu_2GaBO_5 and Cu_2AlBO_5 single crystals. The solid lines are fitting lines using Eq. 3; dashed lines are magnetic contributions due to the magnetically ordered spin subsystem in Cu_2GaBO_5 (red dashed line) and Cu_2AlBO_5 (blue dashed line).

3. Discussion

The unit cell of the investigated ludwigites contains Z = 4 formula units, so the unit cell can contain up to twelve divalent cations (Cu^{2+}, $3d^9$) with spin S = 1/2. Each magnetic Cu^{2+} ion is surrounded by six oxygen ions forming a strongly distorted octahedron. We can identify four types of structurally nonequivalent oxygen octahedra, which correspond to four atomic sites of copper ions. Four types of oxygen octahedra form zigzag walls which are presented in Fig. 7. Interatomic distances between cations and anions are given in Table 3. The obtained here crystallographic parameters are close to the previously published parameters for Cu_2GaBO_5 ludwigites. In addition to Refs. [22,14] we have analyzed the selective distribution of cations on metal sites. The distinctive features of the structures of Cu_2GaBO_5 (**1**) and Cu_2AlBO_5 (**2**) are the selective distribution of Cu, Ga and Al cations (Table 2). M1, M2, M3 and M4 sites in the structure are presented in Fig. 7. M1 and M2 sites are fully occupied by Cu atoms (site-scattering factors = 28.7 and 28.8 epfu); whereas M3 and M4 sites in the structure of **1** are predominately occupied by Ga atoms with less amount of Cu (Ga:Cu = 0.66:0.34 and 0.71:0.29, respectively). M1 and M2 sites are predominately occupied by Cu atoms with significantly less amount of Al (Cu:Al = 0.88:0.12 and 0.86:0.14, respectively); whereas M3 and M4 sites in the structure of **2** are predominately occupied by Al atoms

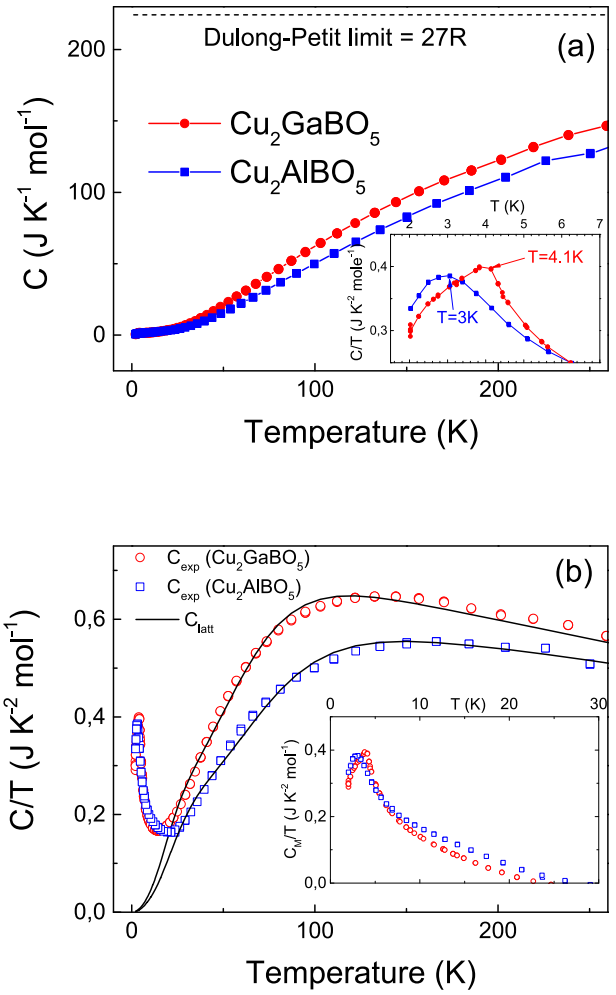


Fig. 5. (a) Temperature dependence of the specific heat $C(T)$ of Cu_2GaBO_5 and Cu_2AlBO_5 measured in zero magnetic field. Inset: Specific heat of Cu_2GaBO_5 and Cu_2AlBO_5 in the temperature range $2\,K \leqslant T \leqslant 10\,K$. (b) Specific heat in representation C/T as a function of T, the black solid line is the fitting curve (see details in the text) Inset: low-temperature magnetic specific heat C_M/T versus T in zero external magnetic field after subtracting the calculated lattice contribution.

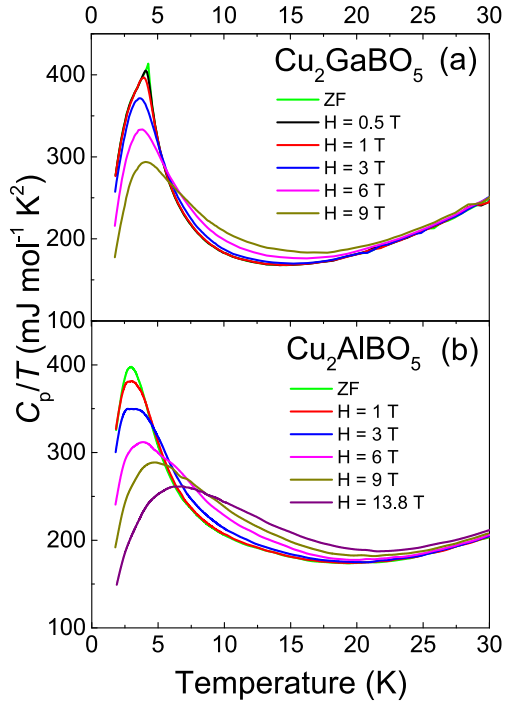


Fig. 6. Magnetic contribution to the specific heat $C_M(T)/T$ of (a) Cu_2GaBO_5 and (b) Cu_2AlBO_5 measured both on field cooling (FC) and in zero magnetic field.

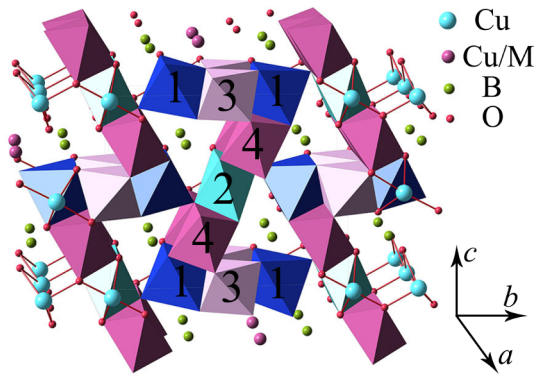


Fig. 7. Crystal structure of Cu_2MBO_5 (M = Ga, Al) ludwigites. Dark blue and light blue octahedrons surround Cu1/M and Cu2/M positions, light magenta and dark magenta octahedrons surround Cu3/M and Cu4/M positions, respectively.

with less amount of Cu (Cu:Al = 0.34:0.66 and 0.33:0.67, respectively). Two sites in the structure **1** Cu_2GaBO_5, which are fully occupied by Cu atoms, form the quasi one-dimensional chains along the crystallographic a-axis that can affect the magnetic properties of the compound. So in the previous work, the estimation of the exchange interactions between copper ions, which are formed these quasi one-dimensional chains, allowed to explain the high value of the linewidth of the electron spin resonance spectra [23].

From magnetic susceptibility measurements (Fig. 1) we can see that for both samples χ can be well fitted by the Curie–Weiss law $\chi = C/(T - \Theta)$ above 50 K, that is confirmed by the linear temperature dependence of the inverse magnetic susceptibility (Fig. 1). The fitting parameters–Curie constant C and Curie–Weiss temperature Θ are summarized in Table 4. The Curie–Weiss temperature Θ is negative, which indicates that exchange interactions between copper spins are predominantly antiferromagnetic in the investigated samples. The effective magnetic moment can be estimated as:

$$\mu_{eff} = \sqrt{3k_B C/N_A} \quad (1)$$

μ_{eff} is equal to $(2.72 \div 2.78)\mu_B$ and $(2.81 \div 2.85)\mu_B$ for the two copper ions in the formula unit of Cu_2GaBO_5 and Cu_2AlBO_5, respectively. Theoretically, the effective magnetic moment of copper ions can be evaluated as:

$$\mu_{eff}(Cu^{2+}) = g\sqrt{N_S S(S+1)} = 2.69\mu_B. \quad (2)$$

Since only the copper spins contribute to the magnetization, we use the value $g = 2.2$ which is characteristic for copper ions in the octahedron environment formed by oxygen ions and $S = 1/2$ for Cu^{2+}, $N_S = 2$ is

Table 4
Fitting parameters of the temperature dependence of the magnetic susceptibility for some compounds of the ludwigite family. The Néel temperature T_N and the fit parameter Θ are given in K; Curie constants are given in emu·K/mol.

	T_N	$\Theta_{\|a}$	$\Theta_{\perp a}$	$C_{\|a}$	$C_{\perp a}$	Ref.
Cu_2GaBO_5	4.1	−69	−74	0.97	0.93	This work
Cu_2AlBO_5	2.4	−47	−58	1.01	0.98	This work
Cu_2GaBO_5	3.4	−68	−54			[12]
$FeMg_2BO_5$	8	−170	−170			[24]

the number of ions with spin S in the chemical formula unit. We can see that the experimentally obtained values of the effective magnetic moments are close to the theoretically predicted ones. As there are 4 inequivalent Cu sites, all of them could have different g-factor values and different magnetic moments. It should be clear that these values refer to some average moments. The effective magnetic moments for Cu_2AlBO_5 is higher than for Cu_2GaBO_5. At low temperatures, we see that the susceptibility χ in Cu_2AlBO_5 approaches a value of 5.58×10^{-2} emu/mol, that is 1.5 times higher than for Cu_2GaBO_5 (Fig. 1). This indicates a more significant paramagnetic contribution from the random distribution of copper ions and defects in the samples.

Magnetic field dependencies of the magnetization in Cu_2GaBO_5 and Cu_2AlBO_5 compounds at temperature 2 K, are presented in Fig. 4. Obtained at T = 2 K M-H curves can be described as a sum of two contributions:

$$M(H) = M_{ord} + M_{disord}. \quad (3)$$

The first term $M_{ord} = \frac{2M_S}{\pi}\tan^{-1}[(H \pm H_C)/H_T]$ is the magnetic contribution [25], which corresponds to the magnetically ordered spin subsystem (dashed lines in Fig. 4), where M_S is the saturation magnetization and H_T is the inner local field of uniaxial anisotropy, H_C is the coercive field. The second term $M_{disord} = \chi \cdot H$ is the magnetic contribution from disordered spins, that means the paramagnetic contribution from defects. The presence of a high amount of paramagnetic defects is proved by the increasing of the magnetic susceptibility below T_N for both compounds (see Fig. 2 and Ref. [21]). Fitting parameters are equal to $M_S = 1\cdot10^3$ emu/mol, $M_S = 0.95\cdot10^3$ emu/mol; $H_T = 2.5$ T, $H_T = 2.8$ T; $\chi = 1.5$ emu/(K·mol), $\chi = 1.4$ emu/(K·mol); and $H_C = 0$ for Cu_2AlBO_5 and Cu_2GaBO_5, respectively. It follows from our description: (i) as we can see from Fig. 4, the relative weight of the ordered component is about 50% from the total magnetic response for both compounds; (ii) the value of the magnetic moment of the ordered phase estimated as $\mu_{eff}^{ord} = M_S/(N_A\cdot\mu_B)$ is equal to $0.18\mu_B/f.u.$ and $0.17\mu_B/f.u.$ for Cu_2AlBO_5 and Cu_2GaBO_5, respectively; that is much lower than the effective moment estimated at temperatures above T_N using Eq. 1; (iii) the weak external magnetic field of 2.5 T and 2.8 T destroys the long magnetic order in Cu_2GaBO_5 and Cu_2AlBO_5, respectively; magnetic spins are polarized along the external magnetic field with increasing of H above these values.

One can suggest that the volume fraction of the ordered state depends on the disorder of the atomic structure, including the selective distribution of metal ions among four nonequivalent positions in the unit cell. Whereas the investigated here and in Ref. [12] samples of Cu_2GaBO_5 ludwigite were obtained in different sample preparation experiments, we can expect the different distribution map of metal ions in these samples, that should affect to their magnetic properties, including the Néel temperature. The antiferromagnetic nature of the phase transition (and the absence of the spin-glass ordering) is proved by the AC magnetization measurements (Fig. 3), where as expected for the AFM structure, the peak is absent in the imaginary part [13].

As we know from X-ray diffraction measurements, there are linear chains of Cu^{2+} ions in the M1 and M2 sites of the investigated sample, located along the crystallographic a-axis (Fig. 7). Typically for 1D antiferromagnetic Heisenberg chains of localized spins the magnetic susceptibility exhibits a maximum at a temperature comparable to the intrachain exchange, as it was in the case of the copper-based compounds $CuTe_2O_5$ [26], $CuTa_2O_6$ [27], $Na_2Cu_2TeO_6$ [28], $Na_3Cu_2SbO_6$ [29], where the temperature dependence of the susceptibility could be approximated using the model of an AFM spin $S = 1/2$ chain [30]. As we can see from Fig. 2, the magnetic susceptibility of Cu_2GaBO_5 and Cu_2AlBO_5 does not exhibit a broad maximum but displays a sharp cusp at 4.1 and 2.4 K, respectively.

Also in contrast to the investigated here bimetallic monomagnetic ludwigites with the temperature of the AFM ordering T_N = 2–4 K and previously investigated $FeMg_2BO_5$ with the Néel temperature $T_N \simeq 8$ K [24] the magnetic phase transition in bimagnetic ludwigites was observed at much higher temperatures: 92 K – for Cu_2MnBO_5 [2], 81–92 K – for $Mn_{3-x}Ni_xBO_5$ [4]. For iron-containing bimagnetic ludwigites (M_2FeBO_5, M = Ni, Cu, Co) it was observed that the ordering temperatures of the Fe^{3+} sub-system in each compound is higher than that of the respective M sub-system [5,31,7,8]. The magnetic phase transition temperature in homometallic magnetic ludwigites is also rather high: 42 K – for Co_3BO_5 [32] and 112 K – the temperature of the partial magnetic transition for Fe_3BO_5, while the whole system of Fe moments become magnetically ordered at T_N = 70 K [33,32].

The investigations of thermodynamic properties showed that at 300 K the specific heat is still considerably lower than the expected high-temperature value $3Rs = 225$ J/(mol·K) for the phonon contribution given by the Dulong-Petit law (Fig. 5), indicating contributions to the phonon-density of states from higher-lying lattice modes. Here, R denotes the gas constant and s the number of atoms per formula unit. We assume that the total heat capacity originates from two different contributions, a lattice contribution C_{latt} due to acoustic and optical phonons and a magnetic contribution C_M corresponding to the thermal population of excited magnetic states. We expect that the magnetic contribution is small compared to the lattice contribution as it was in the case of other copper-based low-dimensional systems [34,35]. The straightforward method to unambiguously extract the magnetic contribution from the experimental data is difficult to realize because a specific heat data for non-magnetic reference material (Mg_2AlBO_5 [36] or Zn_2AlBO_5) is not available. The lattice contribution C_{latt} was approximated following standard procedures [37] with a minimized set of fit parameters only using a sum of one isotropic Debye (C_D) accounting for the 3 acoustic phonon branches and two isotropic Einstein terms (C_{E1}, C_{E2}) averaging the $3s - 3 = 24$ optical phonon branches:

$$C = C_{latt} + C_M,$$
$$C_{latt} = \alpha_D\cdot C_D + \alpha_{E1}\cdot C_{E1} + \alpha_{E2}\cdot C_{E2}. \quad (4)$$

For further reducing the number of free fit parameters, the ratio between these terms was fixed to $\alpha_D : \alpha_{E1} : \alpha_{E2} = 1:4:4$ to account for the $3s = 27$ degrees of freedom per formula unit. For $s = 9$ atoms formula unit, the ratio between acoustical (Debye) and optical (Einstein) contributions is naturally fixed as 1:8. The weight distribution between the optical contributions is chosen in such a way that the degrees of freedom have been equally distributed between the higher Einstein modes. The resulting fit curve (solid line in Fig. 5b) describes the data satisfactorily. For the respective Debye and Einstein temperatures we obtained Θ_D = 166.3 K, Θ_{E1} = 338.4 K, Θ_{E2} = 1009.3 K – for Cu_2GaBO_5 and Θ_D = 189.5 K, Θ_{E1} = 401.3 K, Θ_{E2} = 1108.2 K – for Cu_2AlBO_5. As one can see, the existence of high-frequency modes at 1009.3 K or 1108.2 K agrees well with the fact that the Dulong-Petit value is approached only far above room temperature.

The magnetic contribution to the specific heat C_M was obtained as the difference between the experimentally measured data and the calculated by the Eq. 4 lattice contribution $C_M = C_{exp} - C_{latt}$. The inset in Fig. 5b shows the obtained in such a way the magnetic contribution for zero magnetic field. The temperature dependence of C_M for different values of the applied magnetic field is given in Fig. 6. The magnetic contribution in Cu_2AlBO_5 has the broad maximum, which shifts to high temperatures with increasing magnetic field (Fig. 6a). In some cases this behavior can be attributed to the spin-glass ordering [38–40], if it is accompanied by the feature in the temperature dependence of the imaginary part of AC magnetization. For investigated here compounds we did not observe any features in Fig. 3, so we suggest that such a behavior of the specific heat together with the sharp peak in $\chi - T$ curve (Fig. 2) is due to the AFM transition. The shift of the maximum in the temperature dependence of the magnetic contribution to the specific heat can be due to the partial destruction of the antiferromagnetic order.

For Cu_2GaBO_5 we suggest the presence of one type of the extended phase transition. The transition to a long range AFM begins at T = 4 K and the sample is completely ordered at the temperature $T_N \approx 3$ K. We

attribute this to the random distribution of copper and gallium ions on M3 and M4 positions (see Fig. 7). The long-range magnetic order is easily destroyed by the applied magnetic field larger than 2.5 T, but short-range order regions are preserved. For Cu_2AlBO_5 we suggest the presence of one type of AFM phase transition. Probably, this is the ordering of AFM clusters formed near a nonmagnetic impurity (aluminum). Similar behavior was observed in quasi-one-dimensional magnetic $CuGeO_3$ with impurity and defects [41,42].

4. Summary

Here we presented the investigations of single crystals of Cu_2GaBO_5 and Cu_2AlBO_5 oxyborates with the ludwigite structure synthesized by the flux technique. The distinctive features of the investigated structures are the selective distribution of Cu, Ga and Al cations. The unit cell of Cu_2GaBO_5 and Cu_2AlBO_5 contains four nonequivalent crystallographic sites of metal ions. Two sites in the structure of Cu_2GaBO_5 are predominantly occupied by Ga atoms with less amount of Cu (Ga:Cu = 0.71:0.29 and 0.66:0.34, respectively); whereas other sites are fully occupied by Cu atoms. For Cu_2AlBO_5 all sites are partially occupied by Al and Cu atoms. M1 and M2 sites are predominately occupied by Cu atoms with significantly less amount of Al (Cu:Al = 0.88:0.12 and 0.86:0.14, respectively); whereas M3 and M4 sites are predominantly occupied by Al atoms with less amount of Cu (Cu:Al = 0.34:0.66 and 0.33:0.67, respectively). The magnetic properties of the investigated homomagnetic copper ludwigites are discussed in comparison with known heterometallic bimagnetic ludwigites.

The magnetic measurements showed that the effective magnetic moment and low-temperature magnetic susceptibility for Cu_2AlBO_5 is higher than for Cu_2GaBO_5. This is probably due to changes in the g-factors of copper ions surrounded by more distorted octahedron from oxygen ions.

The analysis of the phonon contribution to the specific heat was performed and the magnetic contribution to the specific heat for both compounds was separated. The Debye and Einstein temperatures were obtained from the analysis of the temperature dependence of the specific heat. The joint analysis of low-temperature data on magnetic susceptibility and magnetic contribution to the specific heat showed that antiferromagnetic clusters which formed near defects in Cu_2AlBO_5 and Cu_2GaBO_5 go into a antiferromagnetic state at $T_N \approx 3$ K. The magnetic phase transitions was started in Cu_2GaBO_5 at $T = 4.1$ K, which can be the transition to the antiferromagnetically ordered state in quasi one-dimensional chain formed by copper ion along the *a*-axis. An external magnetic field above 2.5 T apparently destroys the long-range antiferromagnetic order, but short-range magnetic order is preserved.

CRediT authorship contribution statement

R.M. Eremina: Conceptualization, Methodology, Writing - review & editing, Supervision. **T.P. Gavrilova:** Conceptualization, Methodology, Investigation, Data curation, Writing - original draft, Writing - review & editing. **E.M. Moshkina:** Methodology, Investigation, Resources, Data curation, Writing - original draft, Writing - review & editing. **I.F. Gilmutdinov:** Investigation, Resources. **R.G. Batulin:** Investigation, Resources.

Declaration of Competing Interest

The authors declare that they have no known competing financial interests or personal relationships that could have appeared to influence the work reported in this paper.

Acknowledgments

The reported study was supported by the Russian Foundation for Basic Research (RFBR), grant No 17-02-00953. T.P.G., R.M.E. acknowledge the financial support from the government assignment for FRC Kazan Scientific Center of RAS. D.S.I. acknowledges funding from the German Research Foundation through the Collaborative Research Center SFB 1143 in Dresden (project C03) and the Würzburg-Dresden Cluster of Excellence on Complexity and Topology in Quantum Matter – *ct.qmat* (EXC 2147, project-id 39085490). The XRD and EDX measurements have been performed at the X-ray Diffraction Centre and Centre for Microscopy and Microanalysis of the St. Petersburg State University. The magnetometer studies were performed by the subsidy allocated to Kazan Federal University for the state assignment in the sphere of scientific activities (Project No. 0671-2020-0050).

References

[1] S. Sofronova, E. Moshkina, I. Nazarenko, Yu. Seryotkin, S.A. Nepijko, V. Ksenofontov, K. Medjanik, A. Veligzhanin, L. Bezmaternykh, Crystal growth, structure, magnetic properties and theoretical exchange interaction calculations of Cu_2MnBO_5, J. Magn. Magn. Mater. 420 (2016) 309–316.
[2] E. Moshkina, C. Ritter, E. Eremin, S. Sofronova, A. Kartashev, A. Dubrovskiy, L. Bezmaternykh, Magnetic structure of Cu_2MnBO_5 ludwigite: thermodynamic, magnetic properties and neutron diffraction study, J. Phys. Condens. Matter. 29 (2017) 245801.
[3] E.M. Moshkina, M.S. Platunov, Yu.V. Seryotkin, A.F. Bovina, E.V. Eremin, S.N. Sofronova, L.N. Bezmaternykh, Transformation of structure and magnetic properties of Cu_2MnBO_5 under partial $Mn^{3+} \rightarrow Fe^{3+}$ substitution, J. Magn. Magn. Mater. 464 (2018) 1–10.
[4] L.N. Bezmaternykh, E.M. Kolesnikova, E.V. Eremin, S.N. Sofronova, N.V. Volkov, M.S. Molokeev, Magnetization pole reversal of ferrimagnetic ludwigites $Mn_{3-x}Ni_xBO_5$, J. Magn. Magn. Mater. 364 (2014) 55–59.
[5] M.A. Continentino, J.C. Fernandes, R.B. Guimarães, H.A. Borges, A. Sulpice, J.-L. Tholence, J.L. Siqueira, J.B.M. da Cunha, C.A. dos Santos, Magnetic interactions in the monoclinic ludwigite $Cu_2FeO_2BO_3$, Eur. Phys. J. B 9 (1999) 613–618.
[6] I.I. Nazarenko, S.N. Sofronova, E.M. Moshkina, Magnetic ordering dependence on iron ions distribution in Cu_2FeBO_5 ludwigite, J. Exp. Theor. Phys. 126 (2018) 674–682.
[7] J.C. Fernandes, R.B. Guimarães, M.A. Continentino, H.A. Borges, A. Sulpice, J.-L. Tholence, J.L. Siqueira, L.I. Zawislak, J.B.M. da Cunha, C.A. dos Santos, Magnetic interactions in the ludwigite $Ni_2FeO_2BO_3$, Phys. Rev. B 58 (1998) 287–292.
[8] D.C. Freitas, M.A. Continentino, R.B. Guimarães, J.C. Fernandes, E.P. Oliveira, R.E. Santelli, J. Ellena, G.G. Eslava, L. Ghivelder, Partial magnetic ordering and crystal structure of the ludwigites $Co_2FeO_2BO_3$ and $Ni_2FeO_2BO_3$, Phys. Rev. B 79 (134437) (2009) 1–8.
[9] G.A. Petrakovskiĭ, L.N. Bezmaternykh, D.A. Velikanov, M.S. Malokeev, O.A. Bayukov, A.M. Vorotynov, R. Szymchak, Magnetic properties of the $CuCoAlBO_5$ single crystal, Phys. Solid State 51 (2009) 2486–2491.
[10] N.B. Ivanova, N.V. Kazak, Yu.V. Knyazev, D.A. Velikanov, A.D. Vasiliev, L.N. Bezmaternykh, M.S. Platunov, Structure and magnetism of copper-substituted cobalt ludwigite $Co_3O_2BO_3$, Low Temperature Phys. 39 (2013) 709–713.
[11] L. Bezmaternykh, E. Moshkina, E. Eremin, M. Molokeev, N. Volkov, Yu. Seryotkin, Spin-lattice coupling and peculiarities of magnetic behavior of ferrimagnetic ludwigites $Mn^{2+}_{0.5}M^{2+}_{1.5}Mn^{3+}BO_5$ (M = Cu, Ni), Solid State Phenom. 233–234 (2015) 133–136.
[12] G.A. Petrakovskiĭ, L.N. Bezmaternykh, D.A. Velikanov, A.M. Vorotynov, O.A. Bayukov, M. Schneider, Magnetic properties of single crystals of ludwigites Cu_2MBO_5 ($M = Fe^{3+}, Ga^{3+}$), Phys. Solid State 51 (2009) 2077–2083.
[13] M. Balanda, AC susceptibility studies of phase transitions and magnetic relaxation: conventional, molecular and low-dimensional magnets, Acta Phys. Pol., A 124 (2013) 964–976.
[14] J.A. Hriljac, R.D. Brown, A.K. Cheetham, The synthesis and crystal structures of the related series of aluminoborates: $Co_{2.1}Al_{0.9}BO_5$, Ni_2AlBO_5, and Cu_2AlBO_5, J. Sol. Stat. Chem. 84 (1990) 289–298.
[15] E.M. Moshkina, T.P. Gavrilova, I.F. Gilmutdinov, A.G. Kiiamov, R.M. Eremina, Flux Crystal Growth of Cu_2GaBO_5 and Cu_2AlBO_5, J. Cryst. Growth 545 (125723) (2020) 1–4.
[16] G.M. Sheldrick, SADABS, Univ. Göttingen, Germany, 2007.
[17] CrysAlisPro, Rigaku Oxford Diffraction, Version 1.171.39.35a, 2017.
[18] G.M. Sheldrick, Crystal structure refinement with SHELXL, Acta Cryst. C C 71 (2015) 3–8.
[19] O.V. Dolomanov, L.J. Bourhis, R.J. Gildea, J.A.K. Howard, H. Puschmann, OLEX2: a complete structure solution, refinement and analysis program, J. Appl. Cryst. 42 (2009) 339–341.
[20] A. Linden, Best practice and pitfalls in absolute structure determination, Tetrahedron: Asymmetry 28 (2017) 1314–1320.
[21] R.M. Eremina, E.M. Moshkina, T.P. Gavrilova, I.F. Gilmutdinov, S.N. Sofronova, A.G. Kiiamov, Investigation of the Magnetic Properties of Ludwigites, Bull. Russian Acad. Sci.: Phys. 83 (2019) 912–914.
[22] J. Schaefer, K. Bluhm, Zur Kristallstruktur von $Cu_2M(BO_3)O_2$, (M = Fe^{3+}, Ga^{3+}), Z. Anorg. Allg. Chem. 621 (1995) 571–575.
[23] S. Sofronova, R. Eremina, I. Yatsyk, E. Moshkina, Exchange Interactions in Cu_2AlBO_5 and Cu_2GaBO_5, AIP Conf. Proc. 2218 (040001) (2020) 1–5.

[24] H. Neuendorf, W. Gunßer, Transition from quasi-one-dimensional to spin-glass behaviour in insulating $FeMg_2BO_5$, J. Magn. Magn. Mater. 173 (1997) 117–125.
[25] A.L. Geiler, V.G. Harris, C. Vittoria, N.X. Sun, Quantitative model for the nonlinear response of fluxgate magnetometers, J. Appl. Phys. 99 (2006) 08B316 1-4.
[26] J. Deisenhofer, R.M. Eremina, A. Pimenov, T. Gavrilova, H. Berger, M. Johnsson, P. Lemmens, H.-A. Krug von Nidda, A. Loidl, K.-S. Lee, M.-H. Whangbo, Structural and magnetic dimers in the spin-gapped system $CuTe_2O_5$, Phys. Rev. B 74 (174421) (2006) 1–8.
[27] A. Golubev, R.E. Dinnebier, A. Schulz, R.K. Kremer, H. Langbein, A. Senyshyn, J.M. Law, T.C. Hansen, H.-J. Koo, M.-H. Whangbo, Structural and Magnetic Properties of the Trirutile-type 1D-Heisenberg Anti-Ferromagnet $CuTa_2O_6$, Inorg. Chem. 56 (2017) 6318–6329.
[28] J. Xu, A. Assoud, N. Soheilnia, S. Derakhshan, H.L. Cuthbert, J.E. Greedan, M.H. Whangbo, H. Kleinke, Synthesis, Structure, and Magnetic Properties of the Layered Copper(II) Oxide $Na_2Cu_2TeO_6$, Inorg. Chem. 44 (2005) 5042–5046.
[29] M. Schmitt, O. Janson, S. Golbs, M. Schmidt, W. Schnelle, J. Richter, H. Rosner, Microscopic magnetic modeling for the $S = 1/2$ alternating-chain compounds $Na_3Cu_2SbO_6$ and $Na_2Cu_2TeO_6$, Phys. Rev. B 89 (174403) (2014) 1–10.
[30] D.C. Johnston, R.K. Kremer, M. Troyer, X. Wang, A. Klumper, S.L. Bud'ko, A.F. Panchula, P.C. Canfield, Thermodynamics of spin S = 1/2 antiferromagnetic uniform and alternating-exchange Heisenberg chains, Phys. Rev. B 61 (2000) 9558–9606.
[31] J.C. Fernandes, R.B. Guimarães, M. Mir, M.A. Continentino, H.A. Borges, G. Cernicchiaro, M.B. Fontes, E.M. Baggio-Saitovitch, Magnetic behaviour of ludwigites, Physica B 281–282 (2000) 694–695.
[32] D.C. Freitas, M.A. Continentino, R.B. Guimarães, J.C. Fernandes, J. Ellena, L. Ghivelder, Structure and magnetism of homometallic ludwigites: $Co_3O_2BO_3$ versus $Fe_3O_2BO_3$, Phys. Rev. B 77 (184422) (2008) 1–8.
[33] R.B. Guimarães, M. Mir, J.C. Fernandes, M.A. Continentino, H.A. Borges, G. Cernicchiaro, M.B. Fontes, D.R.S. Candela, E. Baggio-Saitovitch, Cation-mediated interaction and weak ferromagnetism in $Fe_3O_2BO_3$, Phys. Rev. B 60 (1999) 6617–6622.
[34] R.M. Eremina, T.P. Gavrilova, A. Günther, Z. Wang, R. Lortz, M. Johnsson, H. Berger, H.A. Krug von Nidda, J. Deisenhofer, A. Loidl, Magnetization and specific heat of the dimer system $CuTe_2O_5$, Eur. Phys. J. B 84 (2011) 391–395.
[35] Y.V. Lysogorskiy, R.M. Eremina, T.P. Gavrilova, O.V. Nedopekin, D.A. Tayurskii, Vibrational and magnetic properties of crystalline $CuTe_2O_5$, JETP Lett. 100 (2015) 652–656.
[36] A. Bloise, E. Barrese, C. Apollaro, D. Miriello, Synthesis of ludwigite along the Mg_2FeBO_5 Mg_2AlBO_5 join, Neues Jahrbuch für Mineralogie – Abhandlungen, J. Mineral. Geochem. 187 (2010) 217–223.
[37] E.S.R. Gopal, Specific heats at low temperatures, Heywood, London, 1966.
[38] K. Binder, A.P. Young, Spin glasses: experimental facts, theoretical concepts, and open questions, Rev. Mod. Phys. 58 (1986) 801–976.
[39] V. Grinenko, S.-L. Drechsler, M. Abdel-Hafiez, S. Aswartham, A.U.B. Wolter, S. Wurmehl, C. Hess, K. Nenkov, G. Fuchs, D.V. Efremov, B. Holzapfel, J. van den Brink, B. Büchner, Disordered magnetism in superconducting KFe_2As_2 single crystals, Phys. Status Solidi B 250 (2013) 593–598.
[40] P. Skornia, J. Goraus, M. Fijałkowski, A. Ślebarski, Electronic structure and magnetic properties of the magnetically ordered intermediate valent Ce_5RuGe_2, J. Alloys Compd. 767 (2018) 512–521.
[41] S.V. Demishev, A.V. Semeno, N.E. Sluchanko, N.A. Samarin, I.E. Tarasenko, ESR probing of quantum critical phenomena in doped S = 1/2 AF quantum spin chain, Appl. Magn. Reson. 35 (2009) 327–335.
[42] V.N. Glazkov, A.I. Smirnov, O.A. Petrenko, D. McK, A.G. Paul, R.M. Eremina Vetkin, Electron spin resonance in the doped spin-Peierls compound $Cu_{1-x}Ni_xGeO_3$, J. Phys.: Condens. Matter 10 (1998) 7879–7896.